Endoplasmic reticulum localization of the low density lipoprotein receptor mediates presecretory degradation of apolipoprotein B

Donald L. Gillian-Daniel*, Paul W. Bates†, Angie Tebon*, and Alan D. Attie*‡

Departments of *Biochemistry and †Nutritional Sciences, University of Wisconsin, Madison, WI 53706-1544

Edited by Michael S. Brown, University of Texas Southwestern Medical Center, Dallas, TX, and approved January 29, 2002 (received for review October 18, 2001)

Mutations in the low density lipoprotein (LDL) receptor (LDLR) cause hypercholesterolemia because of inefficient LDL clearance from the circulation. In addition, there is a paradoxical oversecretion of the metabolic precursor of LDL, very low density lipoprotein (VLDL). We recently demonstrated that the LDLR mediates presecretory degradation of the major VLDL protein, apolipoprotein B (apoB). Kinetic studies suggested that the degradation process is initiated in the secretory pathway. Here, we evaluated the ability of several LDLR variants that are stalled within the secretory pathway to regulate apoB secretion. Both a naturally occurring mutant LDLR and an LDLR consisting of only the ligand-binding domains and a C-terminal endoplasmic reticulum (ER) retention sequence were localized to the ER and not at the cell surface. In the presence of either of the ER-localized LDLRs, apoB secretion was essentially abolished. When the ligand-binding domain of the truncated receptor was mutated the receptor was unable to block apoB secretion, indicating that the inhibition of apoB secretion depends on the ability of the LDLR to bind to its ligand. These findings establish LDLR-mediated pre-secretory apoB degradation as a pathway distinct from reuptake of nascent lipoproteins at the cell surface. The LDLR provides an example of a receptor that modulates export of its ligand from the ER.

Molecular defects in the low density lipoprotein (LDL) receptor (LDLR) cause Familial Hypercholesterolemia (FH), a condition associated with elevated plasma LDL cholesterol levels (1). Reduced expression, altered ligand binding, or defective transport to the cell surface all lead to a reduction in the functionally effective population of LDLRs at the cell surface.

LDL is produced in the circulation from its precursor, very low density lipoprotein (VLDL). Apolipoprotein B (apoB) is the major protein component of VLDL and LDL. Two observations have suggested that the LDLR might be involved in apoB secretion. First, overproduction of apoB-containing lipoproteins occurs in some cases of FH (2–4). Second, drugs that lower LDL levels by increasing the expression of the LDLR (statins) in many instances have been shown to lower LDL without increasing LDL clearance; i.e., they lower LDL and/or VLDL production (5).

The proportion of apoB that escapes degradation within the secretory pathway primarily determines the rate of VLDL secretion. We recently demonstrated that the presence of the LDLR greatly increases the proportion of apoB subject to presecretory degradation. Our results directly link VLDL overproduction in FH with the loss of the LDLR (6).

Several additional studies support a role for the LDLR in modulating apoB secretion. Increased secretion of VLDL is observed *in vivo* from both $Ldlr^{-/-}$ and transgenic $Ldlr^{-/-}$ mice that overexpress the nuclear form of sterol regulatory element binding protein-1a (SREBP-1a) and *in vitro* in hepatocytes from these animals (7). In contrast, transgenic SREBP-1a animals with a wild-type LDLR accumulate cholesterol and triglycerides intracellularly (7). Mice with phospholipid-transfer protein deficiency produce lower levels of apoB-containing lipoproteins; however, this phenotype is absent in animals lacking the LDLR (8). These findings are consistent with a role for the LDLR in regulating degradation of apoB early in the secretory pathway.

Kinetic modeling of apoB degradation in wild-type and $Ldlr^{-/-}$ mouse hepatocytes predicts multiple pathways of apoB degradation. A presecretory pathway accounts for up to 50% of apoB degradation (6). In the presence of a normal functional LDLR, reuptake of nascent lipoproteins at the cell surface (9) can account for the remaining 50% of apoB degradation (6). To gain insight into the subcellular location of an interaction between apoB and the LDLR, we studied a naturally occurring, transport-defective LDLR mutant. We also studied a recombinant LDLR that consisted of only the ligand-binding domains with an appended ER retention sequence. Both receptor mutants are retained in the ER, and we demonstrate here that ER localization of the LDLR is sufficient to target apoB for degradation.

Methods

Cloning and Mutagenesis of $LDLR_{KDEL}$. Sequences encoding a truncated form of the LDLR ($LDLR_{354}$) (10) were inserted into the plasmid pAdBM5 (Quantum Biotechnologies, Quebec, Canada) at a *Bam*HI restriction site. The amino acid sequence gln lys ala val ***lys asp glu leu*** stop (QKAV***KDEL***stop) was introduced beginning at nucleotide position 5257 (amino acid 355) in $LDLR_{354}$ by annealing and ligating an insert into a unique *Bgl*II restriction site in pAdBM5. Two complementary oligonucleotides encoded this insert: 5′-GATCAGAAGGCCGTGAAAGACGAGCTCTAG-3′ and 5′-GATCCTAGAGCTCGTCTTTCACGGCCTTCT-3′. The sequence encoding $LDLR_{KDEL}$ was subsequently cloned into the pAdtrackCMV plasmid (Quantum Biotechnologies), which contains a cytomegalovirus promoter upstream of the $LDLR_{KDEL}$ sequence to allow for efficient protein expression in mammalian cells. $LDLR_{KDEL}$ was subsequently mutagenized to produce a nonbinding form of the protein. A single amino acid substitution was introduced at position 140 (Ile-140–Asp) by using two complementary oligonucleotides: 5′-CCCACAGCTGGGGGTCGCAGGTGGAGC-3′ and 5′-GCTCCACCTGCGACCCCCAGCTGTGGG-3′ and the Quick Change site-directed mutagenesis protocol (Stratagene).

Mice. Male wild-type (C57BL/6J), C57BL/6J-$Lep^{ob/+}$, and LDLR disrupted ($Ldlr^{-/-}$) C57BL/6J mice (11) were obtained

CELL BIOLOGY

This paper was submitted directly (Track II) to the PNAS office.

Abbreviations: LDL, low density lipoprotein; VLDL, very LDL; LDLR, LDL receptor; apoB, apolipoprotein B; ER, endoplasmic reticulum; FH, Familial Hypercholesterolemia; LSCM, laser scanning confocal microscopy; β-gal, β-galactosidase.

‡To whom reprint requests should be addressed. E-mail: attie@biochem.wisc.edu.

The publication costs of this article were defrayed in part by page charge payment. This article must therefore be hereby marked "*advertisement*" in accordance with 18 U.S.C. §1734 solely to indicate this fact.

from The Jackson Laboratory. Mice were weaned at 3–4 wk, given standard chow and water *ad libitum*, housed on a 12-h dark/12-h light cycle, and killed between 9 and 16 wk of age. Hepatocytes from a C57BL/6J-Lep$^{ob/+}$ mouse were used for immunohistochemical staining of transfected full-length LDLR (see below). The ob mutation is autosomal recessive and the heterozygote (ob/+) is phenotypically wild type (12).

Preparation and Transfection of Primary Mouse Hepatocytes. Hepatocytes were isolated by liver perfusion and cultured in 60-mm dishes as described (6). Alternatively, cells were plated at a density of $\approx 0.25 \times 10^6$ cells/well in a 6-well plate containing glass cover slips for immunohistochemistry. After plating and an overnight incubation, hepatocytes were transfected with 10 μg of various plasmid DNAs and 40 μl of TransIT Insecta transfection reagent (Mirus, Madison, WI) per 60-mm dish. After a 48-h incubation, cells were used for metabolic-labeling studies (below). Alternatively, 2.5 μg of plasmid DNA and 10 μl of TransIT Insecta reagent were used per well in a 6-well plate. Plasmid DNA and transfection reagent were removed after a 12- to 24-h incubation and cells were cultured an additional 12–24 h before fixation for immunohistochemistry.

Immunohistochemistry. Cells were washed once in ice-cold PBS before fixation in 2% paraformaldehyde for 30 min on ice, dried at 65°C for 5 min, permeabilized in 0.1% Triton X-100 in PBS for 30 min on ice, and washed twice with 0.1% Tween-20 in PBS before addition of Ab; Abs were diluted in the same solution. For nonpermeabilized cell controls, hepatocytes were fixed as described and then incubated in 10% FBS in PBS for 30 min on ice before Ab addition. Abs were diluted in 2% BSA in PBS; samples were washed in PBS after Ab incubations. Transfected human LDLR mutants were detected by using the C7 mAb (13) (American Type Culture Collection; 1:2,000 dilution from hybridoma-derived tissue culture medium), where as endogenous LDLR was detected by using a polyclonal rabbit anti-human LDLR$_{354}$ Ab (10) (1:300 dilution). Hepatocytes were incubated with primary Abs on ice for 1 h and washed twice before secondary Ab addition. Polyclonal anti-LDLR Ab was detected by using a Cy3-conjugated sheep anti-rabbit IgG Ab (1:400 dilution; Sigma). C7 anti-LDLR mAb was detected by using a Cy3-conjugated goat anti-mouse IgG Ab (1:200 dilution; Jackson ImmunoResearch). Cells were stained with Con A Alexa 488 (1:4,000 dilution; Molecular Probes) to visualize endoplasmic reticulum (ER). Cells were incubated with secondary Abs at room temperature for 30 min and washed twice with 0.1% Tween-20 in PBS before staining with 0.1 mg/ml 4′,6′-diamidino-2-phenyindole (Sigma) for 5 min at room temperature. Cover slips were mounted with Vectashield (Vector Laboratories).

Samples were visualized by both epifluorescence and laser scanning confocal microscopy (LSCM). Epifluorescence microscopy was performed on a Zeiss Axioskop by using either a 40× or a 63× (n.a.1.4) PlanAPOCHROMAT oil immersion objective lens. Emission/excitation filters for 4′,6′-diamidino-2-phenyindole, FITC, and Cy3 were used. LSCM was performed by using a Bio-Rad MRC1024 LSCM with a MRC1000 confocal imaging system (Bio-Rad) and a krypton/argon laser (model 5470K, Ion Laser Technology, Salt Lake City). All LSCM images were acquired by using a Zeiss Axiovert 100TV microscope and a 63× (n.a. 1.4) PlanAPOCHROMAT oil immersion objective lens. For double-labeling experiments, images were acquired by sequentially exciting at 488 nm and 568 nm to eliminate "bleed through" signal at each fluorescence emission wavelength. A sample with no primary Ab was always included to control for background generated by the secondary Abs. Image processing was carried out by using PHOTOSHOP 6.0 software (Adobe Systems, San Jose, CA).

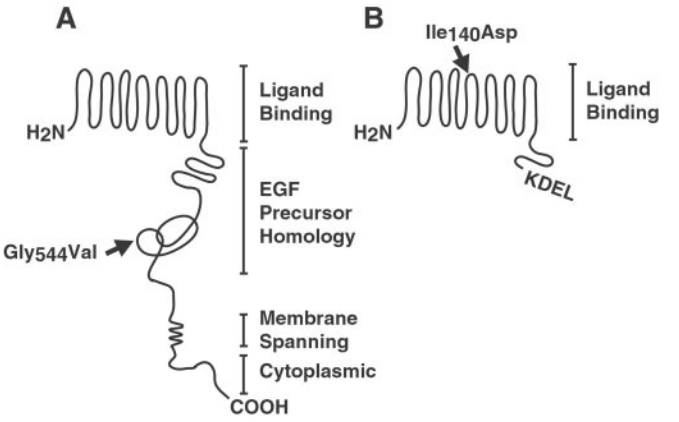

Fig. 1. Cartoon showing structure of the LDLR and mutant forms of the protein. (*A*) Full-length LDLR is depicted along with relevant protein domains. An arrow indicates the relative position of the naturally occurring mutation that created a transport defective LDLR. The mutation is a single amino acid substitution at amino acid position 544 (Gly-544–Val). (*B*) The truncated LDLR is depicted with a carboxyl-terminal KDEL ER retention signal. This receptor consists of the ligand-binding domains and is truncated at amino acid 354 before addition of KDEL. A single amino acid substitution was introduced at amino acid position 140 (Ile-140–Asp; arrow) to create a nonbinding form of the receptor.

Metabolic Labeling of Hepatocytes. Cells were starved for 1 h in methionine/cysteine-free DMEM (GIBCO/BRL) supplemented with 0.2 mM oleic acid (conjugated to BSA; Sigma) before pulse-labeling for 7.5 min in the same medium supplemented with [^{35}S]methionine/cysteine (200 μCi/60 mm dish; EasyTag express protein labeling mix, 1175 Ci/mmol; NEN Life Sciences, Boston, MA). Dishes were washed once with DMEM before a 2 h incubation in chase medium (DMEM supplemented with 10 mM each unlabeled methionine and cysteine and 0.2 mM oleic acid).

Immunoprecipitation and Quantitation of apoB, LDLR, and Albumin. After radiolabeling, cell lysate and media were collected and used for immunoprecipitation as described (6). Abs to apoB (polyclonal, rabbit anti-pig LDL), albumin (polyclonal, rabbit anti-human serum albumin; Sigma), mouse LDLR (polyclonal rabbit anti-LDLR$_{354}$) (10), or human LDLR (C7 mAb; American Type Culture Collection) were added. Radiolabeled protein was separated by SDS/PAGE (14), and specific proteins were visualized by autoradiography. The amount of radiolabeled protein was determined by using PhosphorImager quantitation (Molecular Dynamics; IMAGE QUANT 3.3). All data were normalized to cellular protein (15). The transfected LDLR construct did not significantly alter albumin levels between samples ($P > 0.05$, ANOVA); apoB values were corrected for albumin levels in each sample.

Results

Targeting the LDLR to the ER. We hypothesized that a mutant LDLR, defective solely in transport through the secretory pathway, would decrease lipoprotein secretion by increasing apoB degradation. To test this hypothesis, we measured apoB secretion in the presence of a naturally occurring mutant LDLR that is retained within the ER. This mutation is a single amino acid substitution (Gly-544—Val; hereafter called LDLR$_{GV}$) in the epidermal growth factor homology domain of the receptor (16) (Fig. 1*A*, arrow).

In addition to the naturally occurring mutant LDLR, we constructed a recombinant LDLR with ligand-binding activity that is localized to the ER. We predicted that the epidermal

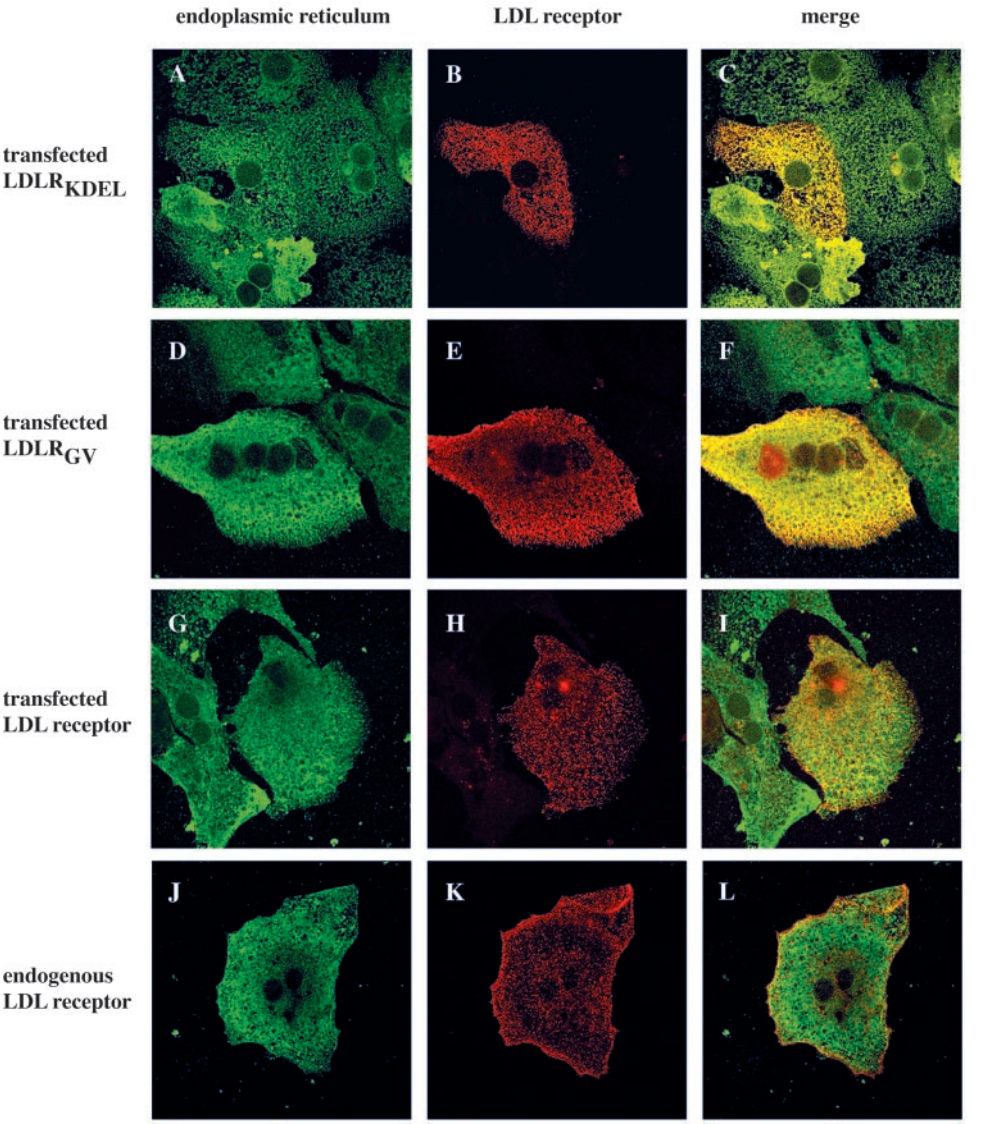

Fig. 2. Transport-defective LDLR mutants are localized to the ER. LSCM was used to visualize endogenous LDLR, transfected LDLR, and mutants there-of in wild-type hepatocytes. (*A*, *D*, *G*, and *J*) Cells were stained with FITC-conjugated Con A Alexa 488 to visualize ER. (*B*, *E*, and *H*) C7 anti-LDLR mAb, detected by a Cy3-conjugated goat anti-mouse IgG Ab, was used to visualize transfected forms of the human LDLR. (*B*) Transfected $LDLR_{KDEL}$. (*C*) Merged image of ER and LDLR shown in separate channels in *A* and *B*, respectively. (*E*) Transfected $LDLR_{GV}$ (naturally occurring mutant; human LDLR). (*F*) Merged image. (*H*) Transfected human, full-length LDLR. (*I*) Merged image. (*K*) Endogenous LDLR visualized by using a polyclonal anti-LDLR Ab detected by a Cy3-conjugated sheep anti-rabbit IgG Ab. (*L*) Merged image.

growth factor homology domain, transmembrane domain, and cytoplasmic tail would be unnecessary for such a protein to mediate apoB degradation. To create this ER-localized LDLR, we used a truncated form of the human LDLR that binds to LDL in a Ca^{2+}-dependent manner (10), analogous to the full-length LDLR (17). This truncated LDLR lacks sequences C terminal to the ligand-binding domains. To arrest the LDLR in the secretory pathway, we attached the amino acid ER-retention sequence, lys-asp-glu-leu (KDEL) (18), at the carboxy terminus (hereafter called $LDLR_{KDEL}$; Fig. 1*B*). This sequence interacts with the KDEL receptor, which in turn recycles KDEL-containing proteins from the Golgi back to the ER (19).

We also constructed a form of the truncated LDLR that is defective in binding to apoB. A single amino acid substitution was introduced into the fourth ligand-binding domain of $LDLR_{KDEL}$ (Ile-140—Asp; hereafter referred to as the nonbinding form of $LDLR_{KDEL}$; Fig. 1*B*, arrow). This substitution essentially abolishes cell surface binding of both LDL and β-VLDL to the LDLR (20), thus reducing receptor-mediated endocytosis and degradation of apoB. This mutant receptor controlled for the possibility that overexpression of the protein in the ER might saturate the KDEL receptor.

Subcellular Localization of Various Forms of the LDLR. We determined the subcellular localization of $LDLR_{GV}$ and $LDLR_{KDEL}$. Primary mouse hepatocytes were transfected with plasmid DNAs encoding the various LDLRs. The expressed proteins were visualized with immunofluorescence staining through LSCM (Fig. 2) and epifluorescence microscopy (Fig. 3). In Fig. 2, the ER was stained with FITC-conjugated Con A (21).

Both $LDLR_{KDEL}$ and $LDLR_{GV}$ colocalized with the ER marker (Fig. 2 *C* and *F*, respectively). In contrast, staining of either transfected full-length human LDLR with C7 mAb (Fig. 2*H*) or endogenous murine LDLR with a polyclonal anti-LDLR

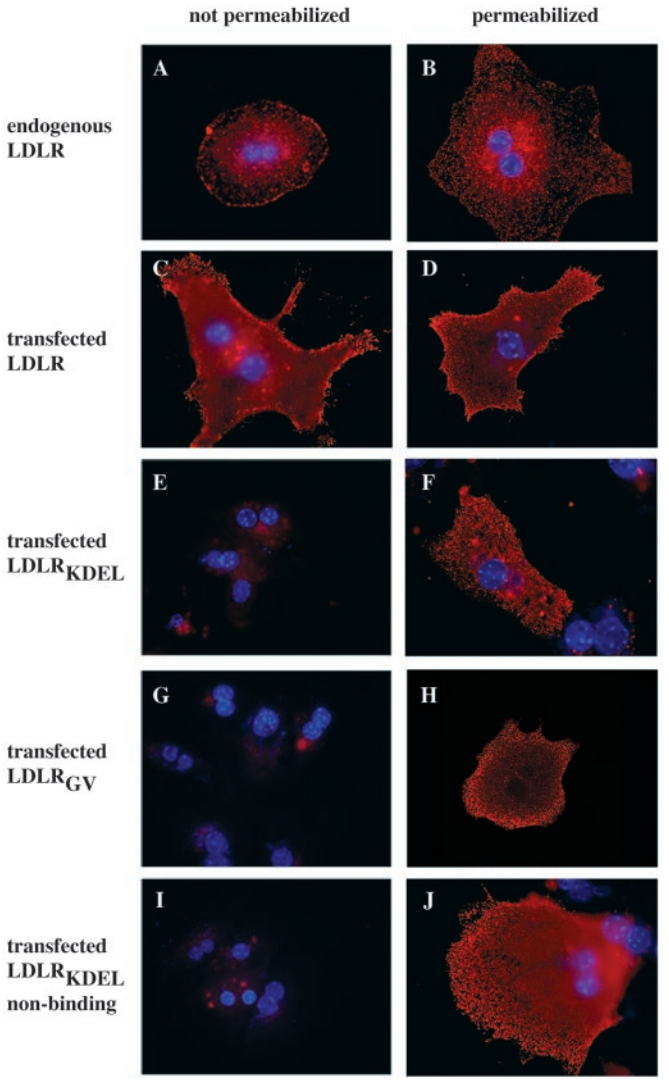

Fig. 3. Transport-defective LDLR mutants are not expressed at the plasma membrane. Epifluorescence microscopy was used to visualize endogenous LDLR, transfected LDLR, and transport-defective LDLR mutants in *Ldlr*$^{-/-}$ (*C–F*) and wild-type hepatocytes (all other panels). (*A* and *B*) Endogenous LDLR was visualized in nonpermeabilized and permeabilized hepatocytes, respectively, using a polyclonal anti-LDLR Ab detected by a Cy3-conjugated sheep anti-rabbit IgG Ab. In the remaining panels, the C7 anti-LDLR mAb, detected by a Cy3-conjugated goat anti-mouse IgG Ab, was used to visualize transfected forms of the human LDLR. Nuclei were stained with 4′,6′-diamidino-2-phenyindole. Transfected LDLR (*C* and *D*), LDLR$_{KDEL}$ (*E* and *F*), LDLR$_{GV}$ (*G* and *H*), and the nonbinding form of LDLR$_{KDEL}$ (*I* and *J*) were visualized in nonpermeabilized and permeabilized hepatocytes, respectively. (*E*, *G*, and *I*) ×40 Magnification; representative of the background levels of staining observed in the entire sample; all other panels are at ×63 magnification. (*H*) LSCM image of transfected LDLR$_{GV}$; 4′,6′-diamidino-2-phenyindole-stained nuclei are not visible in this sample.

Ab (Fig. 2*K*) revealed a punctate pattern that to a large degree did not colocalize with the ER marker (Fig. 2 *I* and *L*, respectively). The C7 mAb used to detect the transfected human LDLRs does not recognize the endogenous mouse LDLR (13). Therefore, only ectopically expressed LDLRs were visible (Fig. 2 *B*, *E*, and *H*). Localization of the nonbinding form of LDLR$_{KDEL}$ was identical to that of LDLR$_{KDEL}$ (data not shown). The presence of the endogenous LDLR did not affect the localization of transfected recombinant LDLRs; the localization of transfected full-length LDLR as well as LDLR$_{KDEL}$ in *Ldlr*$^{-/-}$ hepatocytes was identical to their localization in wild-type hepatocytes (data not shown).

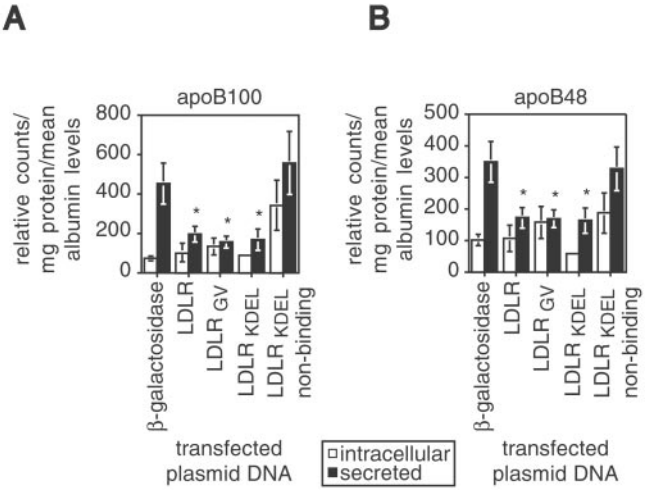

Fig. 4. ApoB secretion is reduced *in vitro* by transport-defective LDLR mutants. (*A*) Intracellular (open bars) and secreted (filled bars) apoB100 levels from *Ldlr*$^{-/-}$ hepatocytes that were transfected with plasmid DNAs encoding various LDLR mutants and β-gal control. (*B*) Intracellular and secreted apoB48 levels from the same samples shown in *A*. Values are mean ± SE ($n = 6$), are expressed as relative counts, and are corrected for milligrams of protein, as well as mean albumin levels in each sample. Samples indicated with an * differ significantly from secreted apoB in cells expressing β-gal ($P \leq 0.01$, Student's *t* test). There was no significant difference in secreted apoB between cells expressing β-gal and those expressing the nonbinding form of LDLR$_{KDEL}$ ($P \geq 0.64$, Student's *t* test).

To confirm that LDLR$_{KDEL}$ and LDLR$_{GV}$ were not expressed at the plasma membrane, we stained hepatocytes that were fixed but not permeabilized. The endogenous LDLR and the transfected full-length LDLR were visible with staining of both nonpermeabilized hepatocytes (Fig. 3 *A* and *C*) and permeabilized hepatocytes (Fig. 3 *B* and *D*). In contrast, staining of LDLR$_{KDEL}$, LDLR$_{GV}$, and the nonbinding form of LDLR$_{KDEL}$ was detected only in permeabilized hepatocytes (compare Fig. 3 *F*, *H*, and *J* to *E*, *G*, and *I*).

ER-Localized LDLRs Abolish ApoB Secretion. To test the prediction that an ER-targeted form of the LDLR can mediate apoB degradation, we carried out pulse–chase experiments in hepatocytes expressing the mutant LDLRs. Primary *Ldlr*$^{-/-}$ hepatocytes were transfected with plasmid DNA encoding either LDLR$_{KDEL}$, the nonbinding form of LDLR$_{KDEL}$, the naturally occurring variant, LDLR$_{GV}$, or as control proteins, both full-length human LDLR, and β-galactosidase (β-gal). ApoB is synthesized in two forms in mouse liver: apoB100, the full-length protein and apoB48, the amino terminal 48% of apoB (22). ApoB100 secretion was reduced by >60% (Fig. 4*A*) and apoB48 secretion reduced by >49% (Fig. 4*B*) in cells expressing LDLR$_{KDEL}$, LDLR$_{GV}$, and full-length LDLR, relative to cells expressing either β-gal or the nonbinding form of LDLR$_{KDEL}$. With transfection efficiencies approaching 50%, this suggests essentially a complete inhibition of apoB secretion in the transfected cells. ApoB secretion was not reduced by ectopic expression of the nonbinding form of LDLR$_{KDEL}$ (Fig. 4 *A* and *B*), establishing that the impairment in apoB secretion requires a functional LDLR ligand-binding domain and is not simply a consequence of protein overexpression in the ER.

Discussion

In this study, we have provided direct evidence that localizing the LDLR to the ER targets apoB for degradation. It confirms

predictions made with pulse–chase kinetic studies of cells expressing or not expressing the endogenous LDLR that the LDLR regulates a step early in the secretory pathway that targets apoB for degradation (6). Because apoB degradation is the primary determinant of the rate of apoB secretion (23), the studies suggest that an ER pool of the LDLR regulates apoB secretion.

Importantly, the LDLR and apoB provide an example of a receptor that modulates export of its ligand from the ER. There are, however, a number of cases in which ligands modulate export of their receptors from the ER. For example, the receptor-associated protein (RAP) facilitates LDLR-related protein (LRP) export by preventing it from interacting prematurely with its ligand, apolipoprotein E (apoE) (24). VLDLR export is impaired in the heart from RAP-deficient mice, possibly through a similar interaction with apoE (25). In addition, other ligand–receptor interactions may come into play because hepatic LRP levels were reduced in $RAP^{-/-}$; $apoE^{-/-}$ animals to the same extent as in $RAP^{-/-}$ animals alone (25). Together these results suggest that ligand–receptor interactions within the secretory pathway may be a more widely used mechanism for regulating protein secretion.

Endogenous LDLR and transfected full-length LDLR were visible with staining of nonpermeabilized hepatocytes (Fig. 3). Low-level staining in the ER (Fig. 2) and staining in nonpermeabilized hepatocytes demonstrated that both transfected full-length and the endogenous full-length LDLR primarily accumulated at the cell surface. Staining of $LDLR_{GV}$, $LDLR_{KDEL}$, and the nonbinding form of $LDLR_{KDEL}$ was detected only in permeabilized cells (Fig. 3), demonstrating that these recombinant LDLRs accumulated in the ER (Fig. 2) without reaching the cell surface.

The localization of both $LDLR_{GV}$ and $LDLR_{KDEL}$ within the ER in the absence of cell surface expression demonstrates that the effects of the LDLR on apoB degradation were initiated within the secretory pathway (Fig. 4). The ER-localized receptors were as effective as full-length LDLR at reducing apoB secretion (Fig. 4). This finding identifies the ER as the site of an initial interaction with the LDLR that results in pre-secretory degradation of apoB. The decrease in apoB secretion did not result in an intracellular accumulation of apoB, consistent with increased posttranslational apoB degradation (6). Because $LDLR_{KDEL}$ and $LDLR_{GV}$ are both localized to the ER (Fig. 2), these forms of the LDLR effectively separate pre-secretory apoB degradation from degradation because of reuptake of nascent lipoproteins at the cell surface.

Ligand binding was essential for the LDLR to target apoB for degradation within the cell, as demonstrated by the absence of an effect of the nonbinding form of $LDLR_{KDEL}$ on apoB secretion (Fig. 4). Therefore, there was a specific interaction between the ER-localized LDLR and nascent apoB-containing lipoproteins. Because apoB secretion was unaffected by the nonbinding form of $LDLR_{KDEL}$, we conclude that the effects of the LDLR on apoB degradation are not caused by protein overexpression in the ER or titration of the KDEL receptor.

ApoB48 lacks the canonical LDLR-binding site (26). The decrease in apoB48 secretion (Fig. 4*B*) in hepatocytes expressing $LDLR_{KDEL}$, $LDLR_{GV}$, and full-length LDLR (6) suggests that either additional sequences in apoB48 or another ligand in the nascent apoB48-containing lipoprotein mediate an interaction with the LDLR in the ER. Interestingly, apoB48 secretion was reduced in phospholipid-transfer protein (PLTP)-deficient mice, but not in PLTP-deficient $Ldlr^{-/-}$ mice (8). A similar reduction in apoB48 secretion was observed in transgenic sterol regulatory element binding protein 1a (SREBP-1a) mice relative to transgenic SREBP-1a; $Ldlr^{-/-}$ animals (7).

Receptor domains are important for protein–protein interactions. For example, the cytoplasmic tail of the LDLR contains an NPXY motif that is required for coated pit-mediated internalization of the receptor (27). LDLR family members also have been implicated in cell-signaling events that require an interaction between sequences in their cytoplasmic tails and intracellular adaptor proteins (28). Multiple cytosolic adaptor and scaffold proteins for LDLR family members have since been identified (29). In addition, a putative LDLR-associated adaptor protein with a phosphotyrosine-binding domain was identified in autosomal recessive hypercholesterolemia (30). Phosphotyrosine-binding domains bind to the consensus NPXY sequence in multiple receptors (31). In light of these results, the finding that ER localization of both full-length $LDLR_{GV}$ and the truncated $LDLR_{KDEL}$ were sufficient to target apoB for degradation is intriguing. The activity of $LDLR_{KDEL}$ demonstrates that the LDLR was able to reduce apoB secretion independent of the receptor epidermal growth factor homology domain, transmembrane domain, and cytoplasmic tail. This result suggests that the cellular degradative machinery may recognize the receptor in complex with apoB, independent of any associated cytosolic adaptor molecules.

There is a processive pathway of lipid acquisition in the secretory pathway during production of the nascent lipoprotein particle (32, 33). Loss of microsomal triglyceride transport protein (MTP) function decreases the amount of triglyceride available for VLDL assembly and results in a concomitant increase in apoB degradation (34). Loss of phospholipid-transfer protein function produces similar results but only in the presence of a functional LDLR (8). We propose that the LDLR binds to apoB within the ER during a period of neutral lipid and/or phospholipid acquisition. When the nascent particle acquires sufficient lipid, its affinity for the LDLR decreases. It is then released and continues through the secretory pathway. This idea is supported by studies demonstrating that particle lipidation state and the resulting lipoprotein conformation affect particle binding to the LDLR (26). LDLR binding of apoB would in effect increase the residence time of the nascent lipoprotein particle within the secretory pathway and in turn make it available for proteolysis. Thus, in the absence of a functional LDLR, smaller VLDL particles containing fewer lipids should be produced. Accordingly, production of small dense VLDL particles is observed in FH (35).

Altered protein export from the ER has been linked to a broad range of diseases (36). For example, mutant MTP results in abetalipoproteinemia, a disease characterized by impaired chylomicron and VLDL production. MTP is required for lipidation of apoB as it translocates into the ER lumen. ApoB is rapidly degraded if it is not lipidated (34). We propose that FH also provides an example of a disease of altered protein export from the ER. In cases of FH that result from a null LDLR mutation, normal pre-secretory degradation of nascent lipoproteins would be diminished because of the lack of a functional LDLR. However, a large fraction of LDLR mutations result in protein that is retained in the ER (37). Our finding that an ER-localized LDLR resulted in apoB degradation suggests that in cases of FH that result from a transport-defective LDLR mutation, lower levels of apoB secretion will be observed and the hypercholesterolemia of these patients would be caused almost entirely by decreased LDL clearance. This idea is supported by the observation that VLDL secretion is not elevated in perfused liver (38) or hepatocytes (39) isolated from the WHHL rabbit, an animal model of FH with a transport-defective LDLR mutation.

The most important observation in this study is that an ER-localized LDLR reduced apoB secretion. The results presented here define presecretory apoB degradation as a process that occurs early in the secretory pathway and depends on LDLR binding. In addition, ligand–receptor interactions within the secretory pathway may be a more universal mechanism for regulating the rate of protein secretion, whether a receptor modulates export of its ligand, as is the case in this article, or vice

versa. Finally, a mechanistic understanding of FH as a disease of altered protein export may ultimately lead to the development of novel treatment strategies.

We thank Kathy Schueler for maintaining and breeding animals used in this study, Jonathan Stoehr for help with statistical analysis, and other members of the Attie laboratory for helpful comments. We also thank Marcia Hebert, Carrie Dickey, and Sarah Crittenden for assistance with immunohistochemistry and microscopy and Adam Steinberg and Robin Davies for assistance with figures. This work was done during the tenure of a fellowship from the American Heart Association, Northland Affiliate (9920482Z to D.L.G-D.). P.W.B. was the recipient of a National Institutes of Health postdoctoral training Grant DK07665-08 (Nutritional Sciences Department). This work was also supported by National Institutes of Health Grant HL-56595 (to A.D.A.).

1. Goldstein, J. L. & Brown, M. S. (1983) in *The Metabolic Basis of Inherited Disease*, eds. Stanbury, J. B., Wyngaarden, J. B., Fredrickson, D. S., Goldstein, J. L. & Brown, M. S. (McGraw–Hill, New York), pp. 1981–1983.
2. Soutar, A. K., Myant, N. B. & Thompson, G. R. (1977) *Atherosclerosis* **28,** 247–256.
3. Packard, C. J., Third, J. L., Shepherd, J., Lorimer, A. R., Morgan, H. G. & Lawrie, T. D. (1976) *Metabolism* **25,** 995–1006.
4. James, R. W., Martin, B., Pometta, D., Fruchart, J. C., Duriez, P., Puchois, P., Farriaux, J. P., Tacquet, A., Demant, T., Clegg, R. J., *et al*. (1989) *J. Lipid Res.* **30,** 159–169.
5. Huff, M. W. & Burnett, J. R. (1997) *Curr. Opin. Lipidol.* **8,** 138–145.
6. Twisk, J., Gillian-Daniel, D. L., Tebon, A., Wang, L., Barrett, P. H. & Attie, A. D. (2000) *J. Clin. Invest.* **105,** 521–532.
7. Horton, J. D., Shimano, H., Hamilton, R. L., Brown, M. S. & Goldstein, J. L. (1999) *J. Clin. Invest.* **103,** 1067–1076.
8. Jiang, X. C., Qin, S., Qiao, C. Kawano, K., Lin, M., Skold, A., Xiao, X. & Tall, A. R. (2001) *Nat. Med.* **7,** 847–852.
9. Williams, K. J., Broci, R. W. & Fisher, E. A. (1990) *J. Biol. Chem.* **265,** 16741–16744.
10. Dirlam, K. A., Gretch, D. G., LaCount, D. J., Sturley, S. L. & Attie, A. D. (1996) *Protein Expression Purif.* **8,** 489–500.
11. Ishibashi, S., Brown, M. S., Goldstein, J. L., Gerard, R. D., Hammer, R. E. & Herz, J. (1993) *J. Clin. Invest.* **92,** 883–893.
12. Coleman, D. L. (1978) *Diabetologia* **14,** 141–148.
13. Beisiegel, U., Schneider, W. J., Goldstein, J. L., Anderson, R. G. & Brown, M. S. (1981) *J. Biol. Chem.* **256,** 11923–11931.
14. Laemmli, U. K. (1970) *Nature (London)* **227,** 680–686.
15. Lowry, O. H., Rosebrough, N. J., Farr, A. L. & Randall, R. J. (1951) *J. Biol. Chem.* **193,** 265–275.
16. Esser, V. & Russell, D. W. (1988) *J. Biol. Chem.* **263,** 13276–13281.
17. Goldstein, J. L., Basu, S. K. & Brown, M. S. (1983) *Methods Enzymol.* **98,** 241–260.
18. Munro, S. & Pelham, H. R. B. (1987) *Cell* **48,** 899–907.
19. Pelham, H. R. B. (1991) *Curr. Opin. Cell Biol.* **3,** 585–591.
20. Russell, D. W., Brown, M. S. & Goldstein, J. L. (1989) *J. Biol. Chem.* **264,** 21682–21688.
21. Cottin, V., Van Linden, A. & Riches, D. W. (1999) *J. Biol. Chem.* **274,** 32975–32987.
22. Greeve, J., Altkemper, I., Dieterich, J. H., Greten, H. & Windler, E. (1993) *J. Lipid Res.* **34,** 1367–1383.
23. Borchardt, R. A. & Davis, R. A. (1987) *J. Biol. Chem.* **262,** 16394–16402.
24. Bu, G. & Schwartz, A. L. (1998) *Trends Cell Biol.* **8,** 272–276.
25. Willnow, T. E., Rohlmann, A., Horton, J., Otani, H., Braun, J. R., Hammer, R. E. & Herz, J. (1996) *EMBO J.* **15,** 2632–2639.
26. Borén, J., Lee, I., Zhu, W., Arnold, K., Taylor, S. & Innerarity, T. L. (1998) *J. Clin. Invest.* **101,** 1084–1093.
27. Chen, W. J., Goldstein, J. L. & Brown, M. S. (1990) *J. Biol. Chem.* **265,** 3116–3123.
28. Trommsdorff, M., Borg, J. P., Margolis, B. & Herz, J. (1998) *J. Biol. Chem.* **273,** 33556–33560.
29. Gotthardt, M., Trommsdorff, M., Nevitt, M. F., Shelton, J., Richardson, J. A., Stockinger, W., Nimpf, J. & Herz, J. (2000) *J. Biol. Chem.* **275,** 25616–25624.
30. Garcia, C. K., Wilund, K., Arca, M., Zuliani, G., Fellin, R., Maioli, M., Calandra, S., Bertolini, S., Cossu, F., Grishin, N., *et al.* (2001) *Science* **292,** 1394–1398.
31. Margolis, B. (1996) *J. Lab. Clin. Med.* **128,** 235–241.
32. Davis, R. A. (1999) *Biochim. Biophys. Acta* **1440,** 1–31.
33. Shelness, G. S. & Sellers, J. A. (2001) *Curr. Opin. Lipidol.* **12,** 151–157.
34. Berriot-Varoqueaux, N., Aggerbeck, L. P., Samson-Bouma, M. & Wetterau, J. R. (2000) *Annu. Rev. Nutr.* **20,** 663–697.
35. Shepherd, J. & Packard, C. J. (1989) *Arteriosclerosis* **9,** Suppl. I, I39–I42.
36. Aridor, M. & Balch, W. M. (1999) *Nat. Med.* **5,** 745–751.
37. Hobbs, H. H., Russell, D. W., Brown, M. S. & Goldstein, J. S. (1990) *Annu. Rev. Genet.* **24,** 133–170.
38. Hornick, C. A., Kita, T., Hamilton, R. L., Kane, J. P. & Havel, R. J. (1983) *Proc. Natl. Acad. Sci. USA* **80,** 6096–6100.
39. Tanaka, M., Otani, H., Yokode, M. & Kita, T. (1995) *Atherosclerosis (Shannon, Irel.)* **114,** 73–82.